

Charge storage in oxygen deficient phases of TiO_2 : defect Physics without defects.

A. C. M. Padilha,^{1,2,*} H. Raebiger,^{1,2} A. R. Rocha,³ and G. M. Dalpian^{1,†}

¹*Centro de Ciências Naturais e Humanas, Universidade Federal do ABC, Santo André, SP, Brazil*

²*Department of Physics, Yokohama National University, Yokohama, Japan*

³*Instituto de Física Teórica, Universidade Estadual Paulista, São Paulo, SP, Brazil*

(Dated: March 4, 2024)

Defects in semiconductors can exhibit multiple charge states, which can be used for charge storage applications. Here we consider such charge storage in a series of oxygen deficient phases of TiO_2 , known as Magnéli phases. These $\text{Ti}_n\text{O}_{2n-1}$ Magnéli phases present well-defined crystalline structures, *i. e.*, their deviation from stoichiometry is accommodated by changes in space group as opposed to point defects. We show that these phases exhibit intermediate bands with the same electronic quadruple donor transitions akin to interstitial Ti defect levels in TiO_2 -rutile. Thus, the Magnéli phases behave as if they contained a very large *pseudo-defect* density: $1/2$ per formula unit $\text{Ti}_n\text{O}_{2n-1}$. Depending on the Fermi Energy the whole material will become charged. These crystals are natural charge storage materials with a storage capacity that rivals the best known supercapacitors.

As our energy requirements grow, and alternative energy sources become an integral part of most countries' energy matrices, energy carriers, in particular charge storage systems play an ever increasing role. Li-ion batteries have played the major role in energy storage up to now [1], but new systems termed supercapacitors [2] have emerged and are becoming more popular. In this case, a number of materials - mainly metal oxide thin films - provide charge storage due to the presence of defects inside its porous structure[3–6].

Titanium oxide is an important wide band gap semiconductor material for applications in photocatalysis [7–9], energy storage [10, 11], and memory devices [12–14]. The stoichiometric phases of this material, TiO_2 -rutile, -anatase, and -brookite are known to present unintentional n-type doping at ambient conditions, owing in part to intrinsic point defects related to oxygen deficiency: oxygen vacancy (V_O) and titanium interstitial (Ti_i) [15, 16]. Further increase in oxygen deficiency leads to the formation of shear planes and consequently a phase transition to the so-called Magnéli phases [17].

A few reports on the thermochemistry [18, 19], electrical properties [20], and electronic structure [21–25] of such systems are available, but the possibility of electronically charging them remains uncharted territory. Such charging becomes relevant as these materials are used as the active media of memristor devices [17, 26] or storage applications [10, 11], and in those cases, the exchange of electrons with a reservoir must be taken into account.

In this letter we study the stability and electronic structure of Ti_4O_7 and Ti_5O_9 Magnéli phases, as well as of the Ti_2O_3 corundum phase, while in contact with a reservoir of electrons. We show that these TiO phases present a series of properties akin to Ti_i -containing TiO_2 -rutile, such as mid gap states and charge state transitions. We show that the intermediate band typical for the Magnéli phases can donate electrons to an electron reservoir, leading to a new electronic phase that resembles

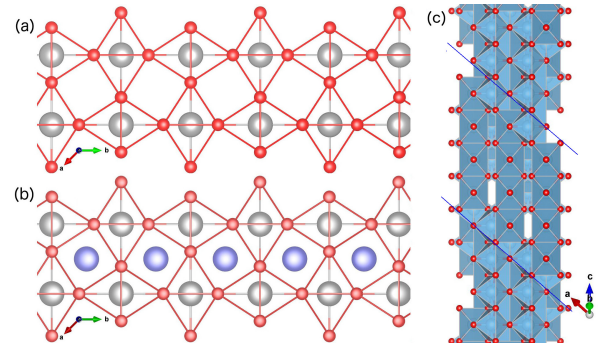


Figure 1. (color online) (a) TiO_2 -rutile structure, (b) and (c) Ti_4O_7 Magnéli phase structures. The oxygen sub net is depicted in red. In (a) and (b) Ti atoms are either gray spheres when in standard rutile sites and blue spheres when in shifted positions while oxygen atoms are red spheres. In (c) the blue lines enclosure the four-units rutile-like chains along the c direction, bounded by corundum-like planes restricted to the (001) planes.

charged defects in a semiconductor, even though they contain no crystallographic defects. The combination of such properties is shown to enable charge storage in these systems in such an efficient way that they can rival the best supercapacitors to date [2].

The Magnéli phases have the general oxygen-deficient chemical formula $\text{Ti}_n\text{O}_{2n-1}$ ($n > 4$). In general, for $n > 37$ the crystal structure is still TiO_2 -rutile, containing point defects or Wadsley defects. Further removal of oxygen (a decrease in n) leads to the reorganization of the crystal into these new crystallographic phases [17, 27]. These phases can be described as being composed of rutile-like chains (edge- and corner-sharing arrangement) of n TiO_6 octahedra units along the c axis bounded by a corundum structure (*i. e.* Ti_2O_3 , composed of face-sharing TiO_6 octahedra) [28–30]. From this point of view, these phases can be interpreted as an ordered combination of TiO_2 -rutile and Ti_2O_3 -corundum

parts. The corundum-like boundaries of the rutile-like region of the Magnéli phases are usually referred to as shear planes. A model structure of these oxygen deficient phases can be obtained from rutile via a shear operation $(121)\frac{1}{2}[0\bar{1}1]$ [19, 25, 31, 32]. This operation can be understood as successive displacements of the atoms in the rutile crystal. All atoms above each (121) plane shifted n times along the c vector from the origin are in turn dislocated in the $[0\bar{1}1]$ direction of the rutile structure. This direction coincides with a lattice vector of the oxygen subnet—*i. e.*, the vector $[0\bar{1}1]$ connects two oxygen atoms in the rutile crystal—, thus it maps the dislocated atoms of that species into atoms of the same species, and finally leaves the lattice positions for oxygen atoms unchanged. Figure 1 shows the structures of TiO_2 -rutile and Ti_4O_7 . From the perspective of (a) and (b) one can see that the oxygen deficiency of such compounds is better described by extra Ti atoms occupying interstitial positions of the TiO_2 matrix, rather than by oxygen atoms missing at specific lattice sites, *i. e.*, oxygen vacancies.

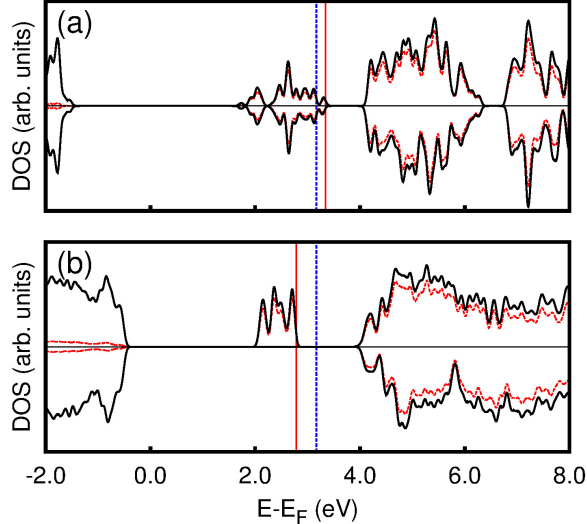


Figure 2. (color online) Projected density of states for (a) Ti_2O_3 and (b) Ti_4O_7 . The spin components are distinguished by the upper and lower panels on each graph. The black full line is the total DOS and the red dashed line represents Ti(d) contribution. Energies are referenced from the last occupied level of the host material (TiO_2) by core-level (Ti 1s) shifts. The full vertical red line indicates the most energetic occupied level of each compound, while the vertical dashed blue line indicates the TiO_2 CMB.

From the electronic point of view, these oxygen-deficient $\text{Ti}_n\text{O}_{2n-1}$ phases present an *intermediate band* [21, 22, 24] slightly below the conduction band minimum (CBM). This is shown by the projected density of states (PDOS) given for Ti_2O_3 and Ti_4O_7 in Figure 2, and for Ti_5O_9 in Figure 4 (upper panel). These DOS show striking resemblance to those observed for isolated defects in TiO_2 [15, 16], and thus, we describe these states to be

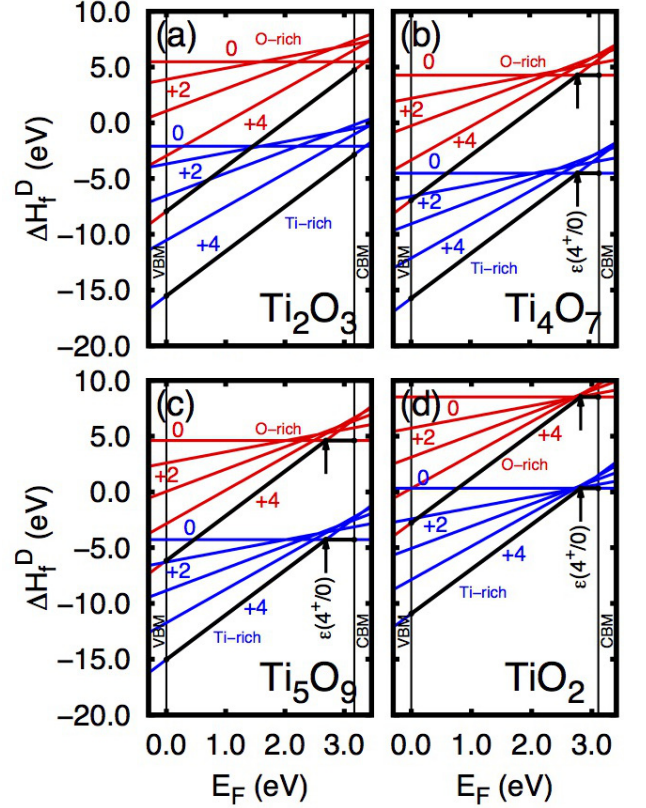
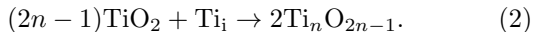
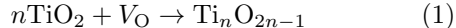


Figure 3. (color online) Formation enthalpies for (a) Ti_2O_3 , (b) Ti_4O_7 , (c) Ti_5O_9 , (d) and Ti_i point defect in TiO_2 -rutile. The Ti_i formation energies shown on (d) are from Ref. [15]. The thick black lines emphasize the lowest energy charge state for each occupation for the entire band gap span, and the transitions from +4 charge state to the neutral charge state in Ti_4O_7 , Ti_5O_9 , and TiO_2 are also featured as $\epsilon(4^+/0)$.

due to the presence of *pseudo-defects* inside the Magnéli phases. As these phases present a high concentration of such *pseudo-defects*, one can think of this intermediate band as the spatially-extended generalization of point defects. Importantly, this *pseudo-defect* band lies close to the TiO_2 -rutile CBM, indicating that its occupation can be tuned by the use of appropriate leads, leading to charging of the material. We investigate this charging process by electronic structure calculations of the first two Magnéli phases Ti_4O_7 and Ti_5O_9 and corundum-phase Ti_2O_3 .

The depletion of oxygen from TiO_2 and the ensuing formation of these oxygen-deficient phases can be described by two processes: (i) either the Magnéli phase is formed by the removal of oxygen and consequently the formation of ordered V_O planes (secant to the c vector, see figure 1) or (ii) from the formation of Ti_i in ordered

planes, *i. e.*,



Our calculations include a reservoir of atoms at constant chemical potential μ_α ($\alpha = \text{Ti}, \text{O}$) and a reservoir of electrons with the chemical potential at E_F . The formation enthalpy ΔH_f^D with respect to TiO_2 as a host material is given by

$$\Delta H_f^D(E_F, \mu, q) = E_D(q) - E_H + \sum_\alpha m_\alpha \mu_\alpha + q(E_F + E_{VBM} + \Delta V), \quad (3)$$

where E_H and $E_D(q)$ are respectively the total energies of the system before (TiO_2) and after ($\text{Ti}_n\text{O}_{2n-1}$) exchanging m_α atoms with the reservoirs. The total energies E_D and E_H are obtained from density-functional calculations performed using the VASP code [33] using the hybrid functional proposed by Heyd, Scuseria, and Ernzerhof (HSE)[34]. The plane wave cutoff is set at 520 eV for all calculations and k-point sampling through the Brillouin zone was performed via the Monkhorst-Pack scheme. For charged systems, the unit cell volume is fixed as that of the uncharged system and atomic positions within the unit cells are relaxed. Our choice is justified by recent experimental results showing the formation of oxygen-deficient crystalline phases inside a TiO_2 matrix [14]. Test calculations where the unit cell was allowed to fully relax were performed, resulting in the same qualitative behavior (see supplementary material for further details). The Fermi energy E_F is given with respect to the VBM of TiO_2 (E_{VBM}), and ΔV is a band-bottom alignment correction used to place all energies at the same reference, obtained from core level shifts [35]. For Ti atoms the $3p4s3d$ electrons were considered as valence electrons whereas the $2s2p$ configuration was considered for O atoms. Core level energies were obtained solving the Kohn-Sham equations for these inner level electrons subjected to a potential given by the pseudopotential method projector-augmented-wave (PAW) scheme [36]. In our calculations the chemical potential of oxygen was obtained from the O_2 molecule while the same quantity for the titanium atom was obtained from a bulk calculation of the hcp structure of metallic Ti.

Typically one uses equation 3 to address the formation enthalpy of defects. Here however we use this methodology to calculate the stability of the *pseudo-defects* in Magnéli phases for different charge states q . The chemical potentials one should use for the expression could be either μ_O for the removed oxygen (Eq. 1; $m_\text{O} > 0$) or μ_Ti for the added titanium (Eq. 2; $m_\text{Ti} < 0$). We choose to discuss only the situation where the Magnéli and Corundum phases are formed via the insertion of Ti atoms (Eq. 2) because the electronic properties of the $\text{Ti}_n\text{O}_{2n-1}$ phases studied here exhibit *pseudo-defect*

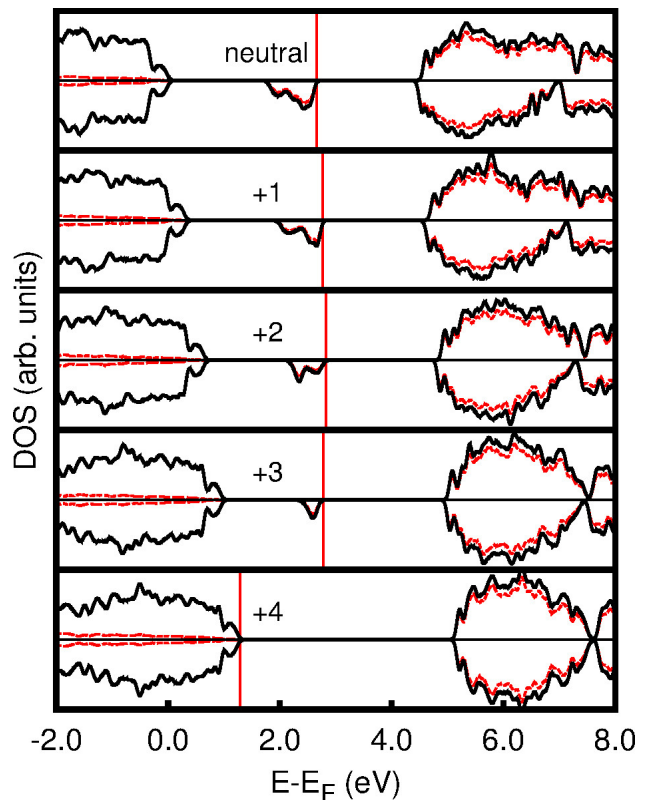


Figure 4. (color online) Projected Density of States (PDOS) for all charge states of Ti_5O_9 . The full black line is the total DOS and the red dashed line represents Ti(d) contribution to the DOS. The two spin components are represented by positive and negative values along vertical axis. The vertical full red line indicates the last occupied electronic level, and the vertical dashed blue line indicates the TiO_2 CBM. Energies are referenced from the last occupied level of the host material (TiO_2 -rutile).

properties as if the material were TiO_2 -rutile doped by Ti interstitial. Moreover, the formation enthalpies for the reaction in Eq. 1 can be obtained by using the oxygen chemical potential μ_O , being the difference in the enthalpy curves in that case just constant shifts to the values presented here; the charge transfer properties remain identical.

Formation enthalpies for the Ti_2O_3 , Ti_4O_7 and Ti_5O_9 structures (when one considers $\alpha = \text{Ti}$ and $m_\alpha = +1$ in equation 3), as well as the same data for the Ti_i in TiO_2 rutile obtained from Lee *et al.* [15] are depicted in Figure 3. O-rich and Ti-rich conditions are obtained by using the boundaries for μ_Ti given by the stability condition of each compound. Notice that Ti_2O_3 presents the full ionized charge state (+4) as the most stable (lowest formation energy) spanning the entire TiO_2 -rutile band gap, while both Ti_4O_7 and Ti_5O_9 present the same trend

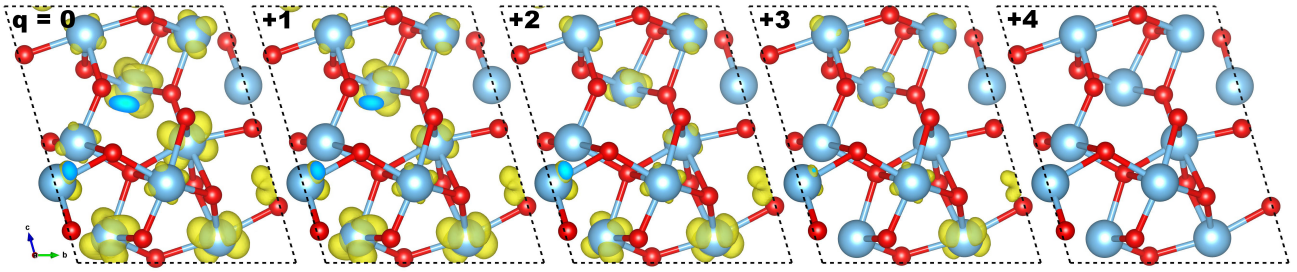


Figure 5. (color online) Real space projection of the *intermediate band* on the PDOS of figure 4, from $E_F - 1.5$ eV to E_F from all charged states with the exception of +4. The isosurfaces are depicted for all charge states, from the neutral case to +4 from left to right. We plot the same isosurface ($10^{-2} e \cdot \text{Bohr}^{-3}$). The +4 charge state presents no intermediate band, the structure is presented only for the sake of completion.

from the VBM up to $\varepsilon(+4/0) = E_{\text{CBM}} - 0.36$ eV and 0.48 eV respectively. The position of $\varepsilon(+4/0)$ marks an abrupt transition from the +4 state to the neutral state. Interestingly this transition lies close to the very same $\varepsilon(+4/0)$ for the isolated Ti_i in TiO_2 -rutile (0.29 eV) [15]. Thus our defect-free $\text{Ti}_n\text{O}_{2n-1}$ structures behave in a fashion similar to TiO_2 with intrinsic defects (Ti_i or V_O). An important distinction must be taken at this point, since the presence of extrinsic defects can lead to different behaviors. For example, nitrogen impurities in the Magnéli phases lead to an electron-hole compensation effect that can significantly alter properties such as the bandgap and photocatalytic activity [37]. We emphasize the fact that we vary the occupation of the *pseudo-defect* induced *intermediate band* in a similar fashion as it is done to mid gap states of isolated defects inside semiconductors. Moreover both Ti_4O_7 and Ti_5O_9 present negative- U behavior [38]. This is also the case of Ti_i point defects inside TiO_2 -rutile [15].

The nature of the charged state in the $\text{Ti}_n\text{O}_{2n-1}$ structures can be understood from the Projected Density of States (PDOS) and real-space projections of selected states. Figures 4 and 5 show this kind of analysis for Ti_5O_9 as a point in case— Ti_4O_7 presented a similar behavior (see supplementary material). The neutral structure shows a midgap *intermediate band* akin to isolated defect states. These states are mostly of $\text{Ti}(d)$ character—as are the unoccupied bands—delocalized over several Ti atoms, as shown in Figure 5. It is known from literature that 3d transition metal related defects exhibit multiple charged states [39, 40] as is the case of Ti_i in TiO_2 -rutile [15]. Recently, such charge transitions have also been observed for extended defects [40]. Here, we show that even perfect crystals that deviate from stoichiometry may exhibit similar charge states. The d orbital rehybridization seen in Figure 5 suggest that these multiple charge states of the *pseudo-defects* in the Magnéli phases are facilitated by a self-regulating response mechanism [39, 41, 42] which also explains why the material does not undergo a Coulomb catastrophe.

To estimate the storage capacity of these Magnéli

phases, we consider a maximum of 4 holes per *pseudo-defect* corresponding to the quadruple donor transition observed, as well as the maximum capacity of the intermediate band to accommodate 4 electrons—two electrons for each of the two V_O 's, or alternatively, four electrons for a single Ti_i , according to the previous discussion. Using this and considering a device operating at a 1 V potential, the theoretical maximum capacitance is approximately 1300 F/g for Ti_2O_3 , 600 F/g for Ti_4O_7 , and 500 F/g for Ti_5O_9 , placing those systems at par with materials used to build supercapacitors. As discussed earlier, by interfacing these oxygen deficient phases appropriate leads, one can control its charge state.

In conclusion, we have performed electronic structure DFT calculations to assess the formation and electric charging of the TiO Magnéli and corundum phases. We show that these materials contain *pseudo-defects*, *i. e.*, they behave akin to Ti_i doped TiO_2 -rutile with a concentration of $1/2$ quadruple donor defects per formula unit $\text{Ti}_n\text{O}_{2n-1}$. These *pseudo-defects* are characterized by an *intermediate band* that can be charged, thus, the material can become charged and used for high-capacity charge storage. We propose that the same behavior shown here for the oxygen deficient TiO phases exists in other semiconductor materials. The required condition is the presence of the *intermediate band* with a large enough density of states, which we expect to be the case in other materials that present stable phases over a wide range of stoichiometries.

This work was supported by FAPESP and CNPq. The support given by Cenapad-SP in the form of computational infrastructure is also acknowledged.

* antonio.padilha@ufabc.edu.br

† gustavo.dalpian@ufabc.edu.br

[1] J. B. Goodenough and K.-S. Park, J. Am. Chem. Soc. **135**, 1167 (2013).

[2] Z. Yu, L. Tetard, L. Zhai, and J. Thomas, Energy Environ. Sci. **8**, 702 (2015).

- [3] W. Sugimoto, H. Iwata, Y. Yasunaga, Y. Murakami, and Y. Takasu, *Ang. Chem. Int. Ed.* **42**, 4092 (2003).
- [4] M. Toupin, T. Brousse, D. Blanger, and D. Be, *Chem. Mat.*, 3184 (2004).
- [5] P. Simon and Y. Gogotsi, *Nature Mat.* **7**, 845 (2008).
- [6] M. J. Young, A. M. Holder, S. M. George, and C. B. Musgrave, *Chem. Mat.*, 1172 (2015).
- [7] A. L. Linsebigler, G. Lu, and J. T. Yates, *Chem. Rev.* **95**, 735 (1995).
- [8] C. Di Valentin, G. Pacchioni, and A. Selloni, *Phys. Rev. Lett.* **97**, 166803 (2006).
- [9] P. Krüger, J. Jupille, S. Bourgeois, B. Domenichini, A. Verdini, L. Floreano, and A. Morgante, *Phys. Rev. Lett.* **108**, 126803 (2012).
- [10] Y. Zhang, X. Pu, Y. Yang, Y. Zhu, H. Hou, M. Jing, X. Yang, J. Chen, and X. Ji, *Phys. Chem. Chem. Phys.* **17**, 15764 (2015).
- [11] S. M. Oh, J. Y. Hwang, C. S. Yoon, J. Lu, K. Amine, I. Belharouak, and Y. K. Sun, *ACS Appl. Mat. Int.* **6**, 11295 (2014).
- [12] G. D. Wilk, R. M. Wallace, and J. M. Anthony, *J. Appl. Phys.* **89**, 5243 (2001).
- [13] D. B. Strukov, G. S. Snider, D. R. Stewart, and R. S. Williams, *Nature* **453**, 80 (2008).
- [14] D.-H. Kwon, K. M. Kim, J. H. Jang, J. M. Jeon, M. H. Lee, G. H. Kim, X.-S. Li, G.-S. Park, B. Lee, S. Han, M. Kim, and C. S. Hwang, *Nature Nanotech.* **5**, 148 (2010).
- [15] H.-Y. Lee, S. J. Clark, and J. Robertson, *Phys. Rev. B* **86**, 075209 (2012).
- [16] A. Janotti, J. B. Varley, P. Rinke, N. Umezawa, G. Kresse, and C. G. Van de Walle, *Phys. Rev. B* **81**, 085212 (2010).
- [17] K. Szot, M. Rogala, W. Speier, Z. Klusek, a. Besmehn, and R. Waser, *Nanotechnology* **22**, 254001 (2011).
- [18] L. Liborio and N. Harrison, *Phys. Rev. B* **77**, 1 (2008).
- [19] S. Harada, K. Tanaka, and H. Inui, *J. Appl. Phys.* **108**, 083703 (2010).
- [20] R. Bartholomew and D. Frankl, *Phys. Rev.* **187**, 828 (1969).
- [21] L. Liborio, G. Mallia, and N. Harrison, *Phys. Rev. B* **79**, 245133 (2009).
- [22] M. Weissmann and R. Weht, *Phys. Rev. B* **84**, 144419 (2011).
- [23] I. Leonov, a. N. Yaresko, V. N. Antonov, U. Schwingenschlögl, V. Eyert, and V. I. Anisimov, *J. Phys. Cond. Mat.* **18**, 10955 (2006).
- [24] A. C. M. Padilha, J. M. Osorio-Guillén, A. R. Rocha, and G. M. Dalpian, *Phys. Rev. B* **90**, 035213 (2014).
- [25] A. C. M. Padilha, A. R. Rocha, and G. M. Dalpian, *Phys. Rev. Appl.* **3**, 024009 (2015).
- [26] F. Pan, S. Gao, C. Chen, C. Song, and F. Zeng, *Mat. Sci. Eng. Rep.* **83**, 1 (2014).
- [27] L. A. Bursill, B. G. Hyde, O. Terasaki, and D. Watanabe, *Phil. Mag.* **20**, 347 (1969).
- [28] M. Marezio and P. Dernier, *J. Sol. State Chem.* **3**, 340 (1971).
- [29] M. Marezio, D. McWhan, P. Dernier, and J. Remeika, *J. Sol. State Chem.* **6**, 213 (1973).
- [30] Y. Le Page and M. Marezio, *J. Sol. State Chem.* **53**, 13 (1984).
- [31] G. J. Wood and L. A. Bursill, *Proc. R. Soc. A* **375**, 105 (1981).
- [32] S. Andersson, D. H. Templeton, S. Rundqvist, E. Varde, and G. Westin, *Acta Chem. Scand.* **14**, 1161 (1960).
- [33] G. Kresse and J. Furthmüller, *Phys. Rev. B* **54**, 11169 (1996).
- [34] J. Heyd, G. E. Scuseria, and M. Ernzerhof, *J. of Chem. Phys.* **118**, 8207 (2003).
- [35] Y.-H. Li, A. Walsh, S. Chen, W.-J. Yin, J.-H. Yang, J. Li, J. L. F. Da Silva, X. G. Gong, and S.-H. Wei, *Appl. Phys. Lett.* **94**, 212109 (2009).
- [36] P. E. Blöchl, *Phys. Rev. B* **50**, 17953 (1994).
- [37] M. Niu, H. Tan, D. Cheng, Z. Sun, and D. Cao, *J. Chem. Phys.* **143**, 054701 (2015).
- [38] G. D. Watkins, *Adv. Sol. State Phys.* **24**, 163 (1984).
- [39] F. Haldane and P. Anderson, *Phys. Rev. B* **13**, 2553 (1976).
- [40] H. Raebiger, H. Nakayama, and T. Fujita, *J. Appl. Phys.* **115** (2014), 10.1063/1.4838016.
- [41] H. Raebiger, S. Lany, and A. Zunger, *Nature* **453**, 763 (2008).
- [42] C. Wolverton and A. Zunger, *Phys. Rev. Lett.* **81**, 606 (1998).